

RADIOISOTOPE PRODUCTIONS FOR MEDICAL USE

A. Hashizume

RIKEN(The Institute of Physical and Chemical Research)
Hirosawa 2-1, Wakoshi, Saitama, 351-01, Japan

Abstract: Many radioisotopes for medical applications are produced by using charged particle induced reactions. The compilation were made for 400 excitation functions and yields for 20 radioisotopes and for impurities. It is realized that the discrepancies exists sometimes between different experiments. The use of monitor reactions is stressed. Suggestion is made to use projectile fragmentation by heavy ion induced reaction to produce carrier free neutron rich isotopes. Some code calculation results are commented.

(medical radioisotopes, excitation function, monitor reaction)

Introduction

Radioisotopes are used for therapeutic and diagnostic purposes. For diagnosis, radioisotopes are served in vivo and/or in vitro. The usefulness of radioisotopes for medical application depends on the decay properties of the radioisotopes and, in vivo use, the behavior of the radioisotopes or their compounds in a body. This behavior depends on physical or mechanical localization, biochemical localization and/or pharmaceutical localization. For example iodine come to thyroid by biosynthesis. This is a biomedical localization. These properties are combined with detection methods such as scintillation scanner, scintillation camera, emission computed tomography(ECT) in which contain positron emission computed tomography(PET) and radionuclide computed tomography(RCT). there are also radionuclide computed tomography(RCT), radiocadiograph(RCG) and/or hepatogram. To have good spatial resolution on the images obtained by these apparatus, special kinds of decay properties are required and good concentration to the objective part in a body is necessary. From this point of view, how to labell the compound by the radioisotopes is also major interest/1/.

In vitro use, There exist many labelled compounds by radioisotopes, and these compounds

have been used for radioassay.

Need of Nuclear Data

In table 1(a), the radioisotopes assigned as the radioisotope for radiopharmaceuticals by law in Japan are listed. Table 1(b) shows other radioisotopes for medical use/2/. The number of radioisotopes for medical application are increasing and here the number exceeds one hundred.

For the production of these radioisotopes, both knowledge of the nuclear structure data and the nuclear reaction data are necessary. Primary important nuclear structure data are the half-lives and absolute emission probability of strongest gamma-ray per decay, as these data are utilized to obtain the excitation function in the stack foil method.

Examining the Evaluated Nuclear Structure Data File(ENSDF), almost of the values of half-lives have good accuracies, but some absolute emission probabilities of gamma-rays per decay for some isotopes have relatively large errors. Table 2 lists some radioisotopes for which we are compiling the excitation functions. The errors of absolute emission probabilities of gamma-rays per decay come from two factors, one is their relative intensity and second is the

Table 1 List of Radioisotopes for Medical use

(a) Radiopharmaceuticals assigned by law		(b) Other Radioisotopes for Medical Use	
Type of Decay	Radiopharmaceuticals	Type of Decay	Radioisotopes*
α -decay	^{222}Rn , ^{226}Ra	α -decay	^{28}Mg , ^{47}Sc .
β^- -decay	^3H , ^{14}C , ^{24}Na , ^{32}P , ^{35}S , ^{42}K , ^{43}K , ^{45}Ca , ^{47}Ca , ^{59}Fe , ^{60}Co , ^{72}Ga , ^{76}As , ^{82}Br , ^{85}Kr , ^{86}Rb , ^{90}Sr , ^{90}Y , ^{99}Mo , ^{111}Ag , ^{132}Te , ^{131}I , ^{132}I , ^{133}Xe , ^{177}Lu , ^{182}Ta , ^{192}Ir , ^{198}Au , ^{199}Au , ^{200}Hg	β^- -decay	^{105}Rh , ^{109}Pd , ^{166}Ho
β^+ -decay	^{11}C , ^{13}N , ^{15}O , ^{18}F , ^{22}Na	β^+ -decay	^{30}P , ^{38}K
Electron capture (+ β^+ -decay)	^{51}Cr , ^{52}Mn , ^{52}Fe , ^{55}Fe , ^{57}Co , ^{58}Co , ^{65}Zn , ^{67}Ga , ^{68}Ga , ^{68}Ga , ^{74}As , ^{75}Se , ^{81}Rb , ^{85}Sr , ^{87}Y , ^{111}In , ^{113}Sn , ^{123}I , ^{125}I , ^{131}Cs , ^{157}Dy , ^{169}Yb , ^{197}Hg , ^{201}Tl	Electron capture (+ β^+ -decay)	^{45}Ti , ^{48}Cr , ^{51}Mn , ^{55}Co , ^{56}Ni , ^{57}Ni , ^{61}Cu , ^{64}Cu , ^{62}Zn - ^{62}Cu , ^{60}Ga , ^{68}Ga , ^{75}Se , ^{75}Br , ^{75}Kr - ^{75}Br , ^{77}Br , ^{82}Br , ^{77}Kr - ^{77}Br , ^{81}Rb - ^{81}mKr , ^{79}Kr , ^{82}mRb , ^{82}Sr - ^{82}Rb , ^{94}Ru , ^{95}Ru , ^{97}Ru , ^{101}mRh , ^{100}Pd , ^{122}Xe - ^{122}I , ^{123}Xe - ^{123}I , ^{127}Cs , ^{128}Ba , ^{129}Cs , ^{167}Tm , ^{203}Pb , ^{211}At , ^{73}Se , ^{153}Gd
Activity with isomer	^{81}mKr , ^{87}mSr , ^{99}mTc , ^{113}mIn	Activity with isomer	^{34}mCl , ^{52}mMn , ^{101}mRh .

* For application of these isotopes, see ref(2).

Table 2 List of nuclear structure data on some radioisotopes for medical application.

Radioisotopes	Half-life		Mode of decay	Principal γ -rays	Nom. error (%)
	values	errors			
^{11}C	20.39	0.02	m	$\text{B}^+(100)$	
^{13}N	9.961	0.004	h	$\text{B}^+(100)$	
^{15}O	122.24	0.16	s	$\text{B}^+(100)$	
^{18}F	109.77	0.05	m	$\text{B}^+(100)$	
^{28}Mg	20.90	0.05	h	$\text{B}^-(100)$	400.6(36 4) 947.8(36 4) 1342.3(54 5) 168.7(99.2)
^{52}Fe	8.275	0.008	h	$\text{B}^+(57)$ $\text{EC}(43)$	1
^{67}Ge	18.7	0.5	m	$\text{B}^+(96)$ $\text{EC}(4)$	167.1(84 3) 4.1
^{67}Ga	3.261	0.001	d	$\text{EC}(100)$	93.3(37.0 7) 184.6(20.4 4)
^{77}Br	57.036	0.006	h	$\text{EC}(99.26)$ $\text{B}^-(0.74)$	239.0(23.9) 520.6(23.1 3)
^{77}Kr	1.24	0.01	h	$\text{B}^+(80)$ $\text{EC}(20)$	129.8(80) 146.4(37.6 10)
^{83}Rb	86.2	0.1	d	$\text{EC}(100)$	520.4(46) 529.7(30.2 14)
$^{82\text{m}}\text{Rb}$	6.472	0.006	h	$\text{EC}(100)$	554.4(62.5 8)
^{111}In	2.83	0.01	d	$\text{EC}(100)$	171.3(90.24 18)0.2 245.4(94.0)
^{123}I	13.2	0.1	h	$\text{EC}(100)$	159.0(83.3)
^{124}I	4.18	0.02	d	$\text{EC}(75)$ $\text{B}^+(25)$	602.7(61)
^{125}I	60.14	0.11	d	$\text{EC}(100)$	35.5(6.66)
^{123}Xe	2.08	0.02	h	$\text{EC}(87)$ $\text{B}^+(13)$	148.9(49)
^{127}Xe	36.41	0.02	d	$\text{EC}(100)$	172.1(23.5 7) 202.9(68)

* Energies(keV) and intensities(%) are shown. For energies, only the digits above 0.1 keV are shown. The errors of intensities are indicated after a space for the last digit. Those which have no errors for relative intensity mean that other gamma-rays are normalized to this gamma-ray.

normalization factor per decay. The latter concerns the emission probability of ground state transition beta-rays and contains usually larger error than that of the relative intensities of gamma-rays if ground state transition of beta-ray exists. In column 5, the energies of gamma-rays, their intensities and their errors of intensities are shown and in column 6 the errors of normalization are cited. In the isotopes listed in Table 1, those which have large errors of normalization are Se-73, Cu-64, Cu-61, Ga-67, Ga-68, Kr-75, I-122, Xe-122, Xe-123 and Cs-127. These isotopes have larger errors than 10% for normalization on intensities of gamma-rays.

Usual techniques to produce neutron rich radioisotopes are utilization of (n, γ) and (n,f) and neutron deficient radioisotopes are made by charged particle reactions. Thermal reactors supply the neutron rich radioisotopes in routine course. Table 3 lists reactor produced medical radioisotopes available from Amersham International presented by Waters/3/. Both nuclear decay schemes and activation cross sections to produce these radioisotopes are now well known and it is said that no problems of purity or supply have been reported.

On Production by Charged Particles

Positron emitters are useful sources of annihilation gamma-rays for PECT. Many radioisotopes which decay by electron capture(EC) are utilized in vivo, because there is advantage free from beta-ray irradiation dose and carrier free radioisotopes can be obtained. These positron emitters and EC isotopes are obtained mainly by charged particle induced reactions.

Integrated cross sections of these reactions are usually measured by stacked foil activation

Table 3 Reactor produced medical radioisotopes available from Amersham International(Waters)/2/.

Radio-isotope	Half-Life	Target Material	Nuclear Reaction
^{24}Na	15.02h	NaCO_3 (Natural)	$^{23}\text{Na}(n,\gamma)^{24}\text{Na}$
^{32}P	14.3d	S (Natural)	$^{32}\text{S}(n,\gamma)^{32}\text{P}$
^{35}S	87.4d	KCl (Natural)	$^{35}\text{Cl}(n,p)^{35}\text{S}$
^{47}Ca	4.54d	CaCO_3 (50% ^{46}Ca)	$^{46}\text{Ca}(n,\gamma)^{47}\text{Ca}$
^{51}Cr	27.7d	Cr (94.6% ^{50}Cr)	$^{50}\text{Cr}(n,\gamma)^{51}\text{Cr}$
^{58}Co	70.8d	Ni (Natural)	$^{58}\text{Ni}(n,p)^{58}\text{Co}$
^{59}Fe	44.6d	Fe_2O_3 (90% ^{58}Fe)	$^{58}\text{Fe}(n,\gamma)^{59}\text{Fe}$
^{75}Se	119.8d	Se(99% ^{74}Se)	$^{74}\text{Se}(n,\gamma)^{75}\text{Se}$
^{85}Sr	64.8d	SrCO_3 (57% ^{84}Sr)	$^{84}\text{Sr}(n,\gamma)^{85}\text{Sr}$
^{89}Sr	50.5d	SrCO_3 (90% ^{88}Sr)	$^{88}\text{Sr}(n,\gamma)^{89}\text{Sr}$
^{90}Y	64.1h	Y_2O_3 (Natural)	$^{89}\text{Y}(n,\gamma)^{90}\text{Y}$
$^{99\text{m}}\text{Tc}$	6.02h	Fission Product	$\text{U}(n,f)^{99}\text{Mo}$ -- $^{99\text{m}}\text{Tc}$
$^{113\text{m}}\text{In}$	99.5m	Sn (80% ^{112}Sn)	$^{112}\text{Sn}(n,\gamma)^{113}\text{Sn}$ -- $^{113\text{m}}\text{In}$
^{125}I	60.0d	Xe (25% ^{124}Xe)	$^{124}\text{Xe}(n,\gamma)^{125}\text{Xe}$ -- ^{125}I
^{131}I	8.04d	Te_2O_3 (Natural)	$^{130}\text{Te}(n,\gamma)^{131}\text{Te}$ -- ^{131}I
^{133}Xe	5.25d	Fission Product	$\text{U}(n,f)^{133}\text{Xe}$
^{137}Cs	30.17	Fission Product	$\text{U}(n,f)^{137}\text{Cs}$
^{192}Ir	74.0	Ir (Natural)	$^{191}\text{Ir}(n,\gamma)^{192}\text{Ir}$
^{198}Au	2.70	Au (Natural)	$^{197}\text{Au}(n,f)^{198}\text{Au}$

method. We collected 400 excitation functions of which reaction products are used for medical applications. Some data of reactions producing impurities for the products have been also collected. These compilations are linked with Nuclear Data Section in IAEA and other Nuclear Data Centers. Fig. 1 shows an example of excitation functions of $^{16}\text{O}(p,\alpha)^{13}\text{N}$. The cross sections were first reported by Whitehead and Foster/4/ followed by Furukawa and Nozaki/5/, however, after the experiments of Gruhle/6/ and McCamis/7/, the resonance structures appeared on the excitation functions in the energy region from 6.5 to 9 MeV of incident energy. An excitation function reported by Gruhle(indicated by a line in the figure) has statistical errors of about $\pm 2\%$ for high energy region and about 15% at the low energy region. The absolute values have errors of about $\pm 9\%$. Same situations are observed in the reactions such as $^{14}\text{N}(p,\alpha)^{11}\text{C}$ and $^{14}\text{N}(d,n)^{15}\text{O}$.

^{18}F is usually produced by $^{18}\text{O}(p,n)^{18}\text{F}$ or $^{20}\text{Ne}(d,\alpha)^{18}\text{F}$ reactions. Lagunas-Solar have

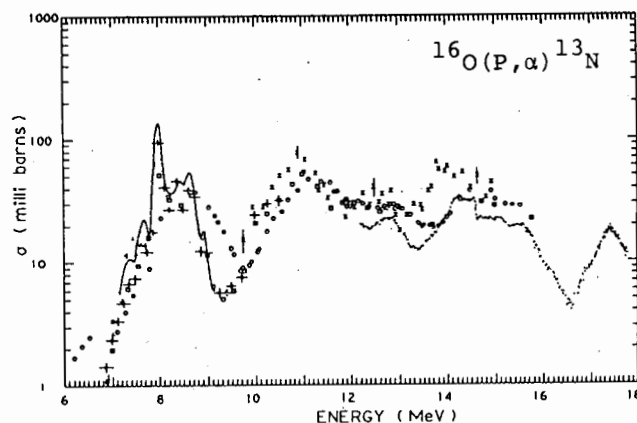


Fig. 1 Excitation functions for the $^{16}\text{O}(p,\alpha)^{13}\text{N}$

studied recently the ^{18}F producing cross-sections by bombarding Na, Mg and Al by protons/8/. The incident energy range studied is relatively high, that is, 20 to 70 MeV. As shown in Fig 2, it was found that $\text{Na}(p,x)^{18}\text{F}$ have broad peak near 40 MeV and the cross section is the largest in the three kinds of targets. The thick target yield in the energy range from 67 to 22 MeV accounts for 88 mCi/uAh which is comparable to the yield of the $^{18}\text{O}(p,n)^{18}\text{F}$ reaction where incident proton energy is 90 Mev and target thickness is 87 MeV and yield is 90 mCi/uAh /9,10/.

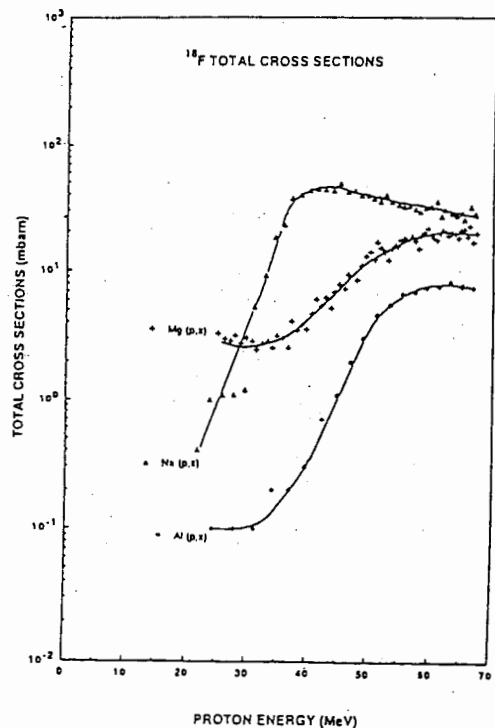


Fig. 2 Total cross sections as a function of proton energies for the production of F-18 from Na, Mg, and Al (Lagunas-Solar /7/).

The positron-emitting ^{52}Fe ($T_{1/2}$ 8.3hr) has been recognized as a useful agent for bone marrow imaging in studying the erythropoietic tissue or other metabolic processes. Other iron isotopes such as ^{55}Fe and ^{59}Fe are not suitable for this purpose because of that their half-lives are too long and the energies of accompanying gamma-rays are too high or low. ^{52}Fe is also used as the parent nuclide for the ^{52}Fe - ^{52}Mn generator system.

The excitation functions to produce ^{52}Fe are typical case where many reaction type have been

Table 4 List of reaction thypes studied for the production ^{52}Fe .

Particle	Reaction	Energy(peak) (MeV)	σ_{max} (mb)	Ref. Author
p	$^{55}\text{Mn}(p,4n)$	40 - 73(54)	1.4	(11) K.Suzuki
	$^{54}\text{Fe}(p,p2n)$	33 - 44(45)	1.4	(12) R.Michel
	$^{54}\text{Fe}(p,t)$	18 - 23	0.3	(13) B.L.Cohen
	$^{54}\text{Fe}(p,dn)$	33 - 60(45)	4	(14) I.R.Williams
	$^{59}\text{Co}(p,\text{sp.11})$	59 - 98(77)	0.44	(15) R.A.Sharp
	$^{58}\text{Ni}(p,\text{ap}2n)$	42 - 56	1.8	(16) S.Tanaka
^3He	$^{52}\text{Cr}(^3\text{He},3n)$	23 - 44(35)	5	(17) M.V.Greene
α	$^{59}\text{Co}(\alpha,3p8n)$	113 - 170	0.26	(18) R.Michel
	$^{54}\text{Fe}(\alpha,\alpha 2n)$	38 - 40	0.34	(19) S.Tanaka
^6Li	$^{54}\text{Fe}(^6\text{Li},X)$	55 - 94	4.8	(20) J.Jastrzebski

studied. Table 4 shows reaction types of which excitation function have been studied. For each reaction type, only one excitation curve has been reported. Other than excitation functions, 23 cases of production yields for ^{52}Fe have been reported.

Figure 3 shows a comparison of relatively recent results of $^{76}\text{Se}(p,n)$, $^{76}\text{Se}(p,2n)$ and $^{76}\text{Se}(p,3n)$ reactions. The agreement is good but their exists some systematic trend on absolute value of cross sections between Groningen and Julich groups/21/.

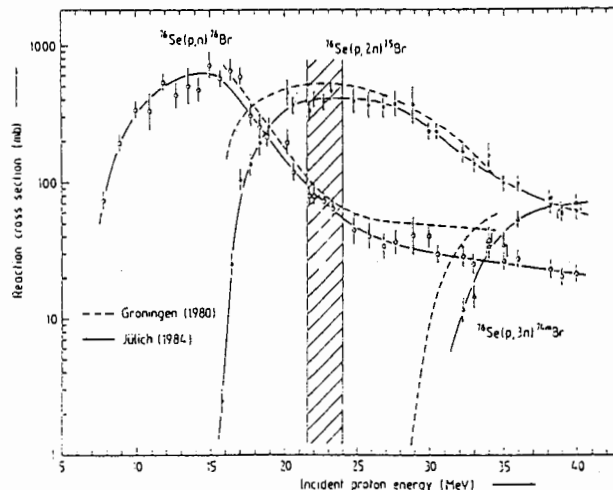


Fig. 3 Excitation functions of (p,xn) reactions on 96.5 % enriched ^{76}Se (Kovacs /20/).

The ^{123}I is an example where its production methods have been well studied. The reaction types of routine production utilize $^{124}\text{Te}(p,2n)^{123}\text{I}$, $^{127}\text{I}(p,5n)^{123}\text{Xe}$, $^{123}\text{Te}(d,n)^{123}\text{I}$, $^{121}\text{Sb}(\alpha,2n)^{123}\text{I}$, $^{123}\text{Sb}(\alpha,4n)^{123}\text{I}$, and $^{122}\text{Te}(\alpha,3n)^{123}\text{Xe}$ reactions. On the $^{127}\text{I}(p,5n)$ reaction, there are five reports for the excitation functions. The status is shown in Fig. 4. The differences of the cross sections at peak values about 55 Mev become more than 50 %. The recent results by Lagunas-Solar/26/ agree to those of Paans/23 /. However there are some discrepancies between the results of Lagunas-Solar and those of Syme who measured also higher energy region.

For $^{124}\text{Te}(p,2n)^{123}\text{I}$ reaction, very high enriched isotopes of ^{124}Te is used for routine

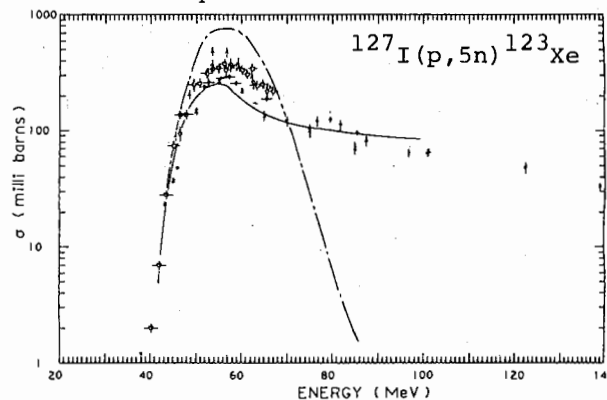


Fig. 4 Excitation functions for the $^{127}\text{I}(p,5n)^{123}\text{Xe}$ reaction. The compound (dashed dotted line) and precompound (line) process calculated by Alice code are shown. Experimental points are taken from ref/21, 22, 23, 24 and 25/.

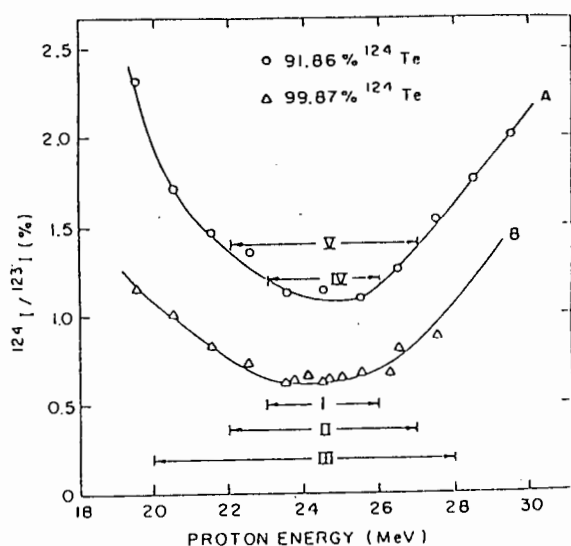


Fig. 5 The impurity of ^{124}I to ^{123}I , 3 h post-irradiation after 1-3 h irradiations at 10-13 uA on 87-160 mg/cm² of ^{123}Te (Kondo /27/).

production. As shown in Fig. 5, employing the 99.87 % isotopically enriched target of thickness 421 mg/cm² (8 MeV for proton), the ratios ^{124}I to ^{123}I is below 1 % which cannot be attained by 91.88 % enrichment/27/. It is noted that the impurity given changes as the time elapses after the end of bombardment and after chemical separation. Fig. 6 shows an example of change of impurity with time/28/. In case of ^{123}I , because of the influence of 529 keV gamma-ray with 1.08 % abundance in the decay, there is an argument that the resolution of images is not influenced until the presence of ^{123}I activity becomes 4.5 %. In general, the percentage of impurities should analyze dynamically, that is, with function of time.

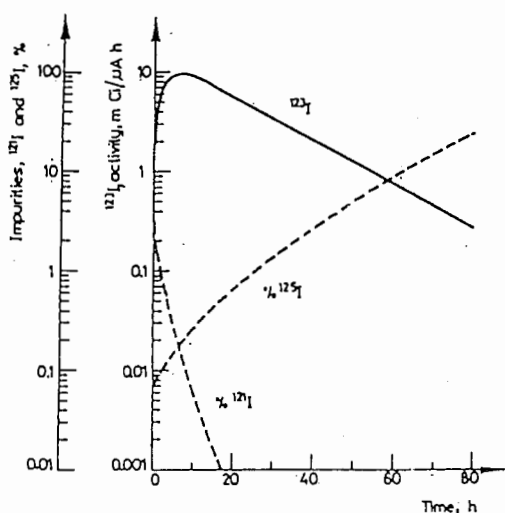


Fig. 6 ^{127}I thick target yields and impurities for deuteron induced reactions (64 MeV $\leq E \leq$ 78 MeV) on NaI, showing the change of impurity percentages to those of ^{123}I (Weinrich /28/)

Monitor Reactions

As illustrated in the figures of excitation functions, there exist, sometimes, discrepancies between reported excitation functions from different authors. One of the reason of these

discrepancies would come from the errors of beam intensity measurements. In this respects monitor reactions should be useful in stacked foil activation methods. The ideal monitor reaction should satisfy the following conditions: 1) The elements should be isotopically pure or disturbances of quantitative determination of reaction product caused by other isotope products are small, 2) The absolute cross sections should be known accurately in wide range of energies of incident particles, 3) The cross sections should change smoothly as incident particle energies increase, 4) The cross sections to other reaction channels should be small, 5) The effects of secondary particles induced by primary reactions should be small, 6) The half-life of reaction product should not be too short or very long as compared to irradiation time, 7) The target foil should be obtained without difficulty, 8) The target should be stable during the irradiation. The elements which have low melting point should be avoided and 9) The activity of reaction products can be determined accurately and easily. The emitting probability of detecting radiation should be accurately known.

In table 6, the types of monitor reaction employed for the measurements of excitation functions whose product is useful for medical applications.

Table 5 Monitor reaction list for the measurements of cross sections of the reactions which produce medical radioisotopes.

Kinds of reactions	Energy region (MeV)	Ref. of reaction employing monitor
$^{12}\text{C}(p, pn)^{11}\text{C}$	21 MeV-300 GeV	(30)
$\text{Al}(p, x)^7\text{Be}$	118-800	(31)
$\text{Al}(p, x)^{22}\text{Na}$	82-800	(31)
$\text{Al}(p, x)^{24}\text{Na}$	70-190	(32), (33)
$^{63}\text{Cu}(p, n)^{63}\text{Zn}$	3 MeV-11.5 GeV	(34), (35)
$^{63}\text{Cu}(p, 2n)^{62}\text{Zn}$	16-33	(35), (36)
$^{65}\text{Cu}(p, n)^{65}\text{Zn}$	3-100	(37)
$^{65}\text{Cu}(p, pn)^{64}\text{Cu}$	23-102	(36)
$^{65}\text{Cu}(p, 4n)^{62}\text{Zn}$	34-100	(36)
$^{27}\text{Al}(d, p\alpha)^{24}\text{Na}$	11-28	(34), (37)
$^{51}\text{V}(d, 2n)^{51}\text{Cr}$	5-90	(38)
$^{56}\text{Fe}(^3\text{He}, p2n)^{56}\text{Co}$	18-29	(35)
$^{56}\text{Fe}(^3\text{He}, pn)^{57}\text{Co}$	6-29	(35)
$^{56}\text{Fe}(^3\text{He}, 2n)^{57}\text{Ni}$	6-29	(35)
$\text{natTi}(^3\text{He}, X)^{48}\text{V}$	5-130	(34), (39)
$^{27}\text{Al}(\alpha, 2p)^{29}\text{Al}$	15-152	(34)
$^{27}\text{Al}(\alpha, ^7\text{Be})^{24}\text{Na}$	40-103	(37)

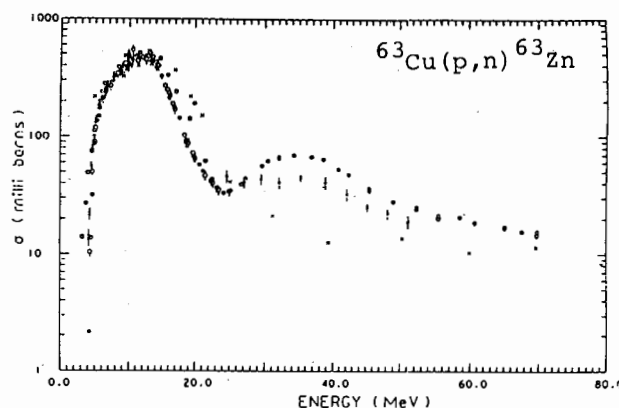


Fig. 7 The excitation function for the $^{63}\text{Cu}(p, n)^{63}\text{Zn}$ reaction.

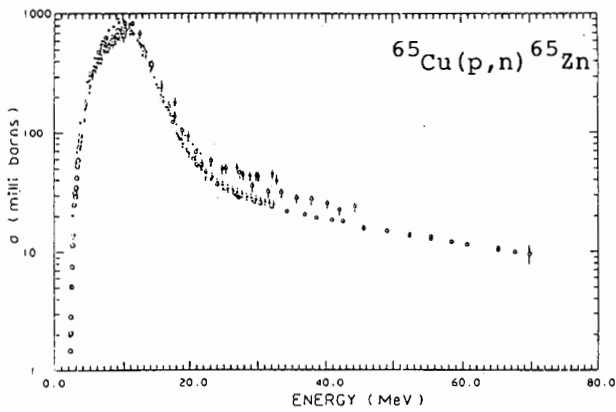


Fig. 8 The excitation function for the $^{65}\text{Cu}(p,n)^{65}\text{Zn}$ reaction.

Historically, since the evaluation work done by Cumming/29/, many absolute measurements have been done for the $\text{C}(p,pn)^{11}\text{C}$ reaction. The smallest cited error is 3% and almost measurements has been done with accuracy of 5%. However, $^{12}\text{C}(p,pn)^{11}\text{C}$ reaction have Q-value of -18.71 MeV and it is relatively difficult to obtain a thin and strong target which resists the beam intensities. About the monitor to produce medical isotopes, copper and aluminum targets are often used, being these substances also served as a energy degrader. The situation are shown in Fig. 7 and 8 for $^{63}\text{Cu}(p,n)^{63}\text{Zn}$ and $^{65}\text{Cu}(p,n)^{65}\text{Zn}$. It is necessary to start evaluation for some of the monitor reactions.

Other reaction types

Usual incident energy of charged particles for the production of medical isotopes are several tenth MeV at maximum. In this energy range, the reactions through compound and precompound processes are predominant except target nuclei in the region of low mass number where direct process often predominates. However the incident energy of several hundredth MeV protons inducing spallation of targets are also utilized combining with a mass separator. Table 6 shows a list of target and cross sections with high energy protons presented by Beyer/41/. Because of long range of protons, yields are high as cross sections are order of several tenth milli-barns.

High energy neutrons from fast bleeder reactor and 14 MeV neutrons/42/ are also utilized for the production of medical isotopes. In FFTF, ^{153}Gd has been made by the decay product of ^{153}Eu by a fast reactor

Though it is rarely used, the photo-reactions are sometimes used. This reaction has advantage to make carrier free neutron rich isotopes, though chemical processing of large value of target make difficult for daily use. The yield of many photoreactions have been examined by Masumoto/43/.

There is a possibility to produce ^{28}Mg and ^{42}Ar - ^{42}K generator by the $^{26}\text{Mg}(t,p)$ and $^{40}\text{Ar}(t,p)$ reactions by a compact cyclotron/44/. However the acceleration of tritium poses another radiation hazard problem.

In RIKEN, a high energy heavy ion accelerator, a four sector cyclotron, are now in operation. A group is studying fragmentations of projectiles. This reaction is different from usual heavy ion reactions which pass through compound and/or precompound processes. The

Table 6 Summary of spallation reaction cross-section data for the radioisotopes in medical use. The proton energy was limited to the 500 MeV region (Beyer/41/).

radio-isotopes	Targets	E(p) (MeV)	Cross-sections(mb) values errors	
^{82}Sr	Zr	590	19	4
	Nb	590	22	4
	Mo	590	15	3
	Mo	800	24.5	0.8
	Mo	800	23	1
^{85}Sr	RbBr	800	2.1	0.2
	Mo	800	48	0.7
^{123}Xe	Mo	800	50	2
	La/Cu	590	36	5
^{125}Xe	La/Cu	590	45	6
	I	660	3.8	0.4
	Cs	660	29.3	1.7
	Ba	660	26	4
	La	660	31.9	1.6
^{127}Xe	La/Cu	590	57	9
	La/Cu	590	43	9
^{123}I	I	660	6.6	0.5
	Cs	660	45	0.5
	Ba	660	38	6
^{167}Tm	La	660	47.7	3.9
	La/Cu	590	53	11
^{168}Tm	La/Cu	600	51	7
	La/Cu	590	57	6
^{211}Rn	La/Cu	590	57	9
	La	800	51	3
	Lu	590	56	6
	Hf	590	51	10
	Ta	590	49	7
^{211}At	W	590	49	7
	Lu	590	5	1
	Hf	590	6	1
^{211}At	Ta	590	0.8	0.4
	W	590	0.4	0.2
^{211}At	Th	660	13	6
	Th	660	18.2	2.2
^{211}At	U	660	5.2	1.4
	U	660	5.2	1.4

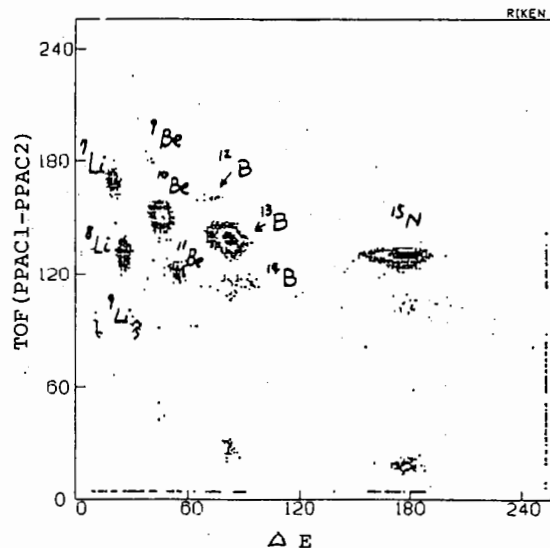


Fig. 9 Spectrum of projectile fragments when 46 mg/cm^2 Be target was bombarded by $42 \text{ MeV/u } ^{15}\text{N}$ ions.

angular distributions of the fragments are strongly forward peaked. Figure 9 and 10 show examples of charge and mass distribution when Be targets are bombarded by $42 \text{ MeV/u } ^{15}\text{N}$ and $28 \text{ MeV/u } ^{40}\text{Ca}$. These distributions were obtained by the combination of magnets, position sensitive silicon detectors and a time of flight technique. By choosing heavy ion projectile and its energy,

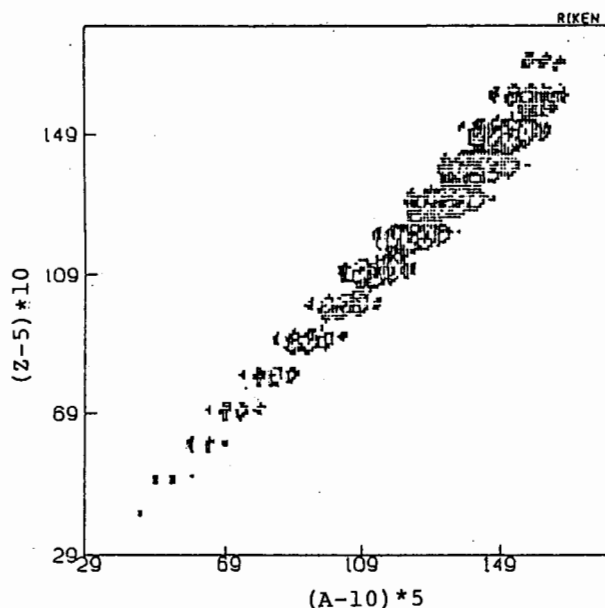


Fig. 10 Spectrum of projectile fragments when $^{23}\text{Mg/cm}^2$ Be target was bombarded by 28 MeV/u ^{40}Ca .

the neutron rich carrier free radioisotopes can be obtained by this methods. These isotopes would be useful for the radioassay in medical and biological use in vitro. We are also constructing an on line mass separator(ion guided type).

Comparison with Some Model Codes

Many version of codes such as ALICE, STAPRE, GNASH are used for the calculation of cross sections induced by charged particle incident reactions. At IAEA consultants' meeting on data requirements for medical radioisotope production, Blann made a comment on results of Alice code(Weisskopf formula+hybrid model) calculation around mass region of 50 /45/. The incident particles were p, d, t and a. Their energy ranges cover up to 200 MeV /46/. For the proton induced reactions, the shapes of the calculated excitation functions are in quite good agreement with data over the entire energy range, giving a good estimate of the optimum bombarding energies. The absolute cross sections are also in quite good agreement with experimental data, except for yields of isotopes near Ni and Co where closed shell effects become important. For deuterons and tritons, with the exception of one neutron transfer reaction channel, the calculation reproduces the shape and absolute cross sections. Blann suggested the estimation of impurities can be made by calculations when there is a lack of the experiment. Figure 10 and 11 show some version of the comparison between experiments and calculations.

A computer code, OSCAR, has been made by Hata and Baba/47/. This code calculates the stopping power, excitation functions and production yields. If an experimental excitation function is not available, it calculates the excitation function from Alice code. Figure 8 shows that some results of calculation of Alice were compared with those of experiments at peak values. It is shown that about 75 % fall in the line of factor of two. In the region of mass number 60, there are many points which deviate from the factor. These points reflect the effect

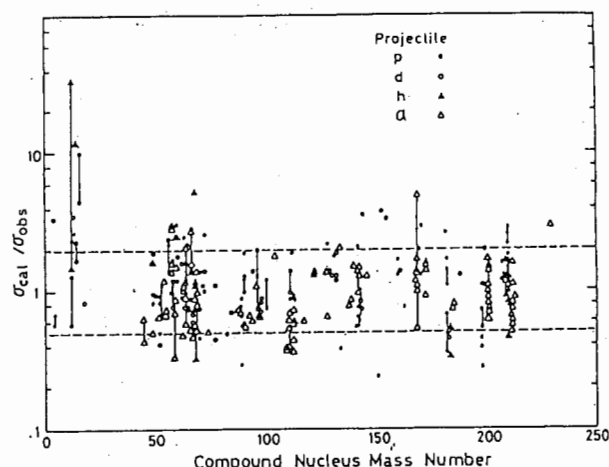


Fig. 11 Ratios of experimental and calculated cross sections at peak of the excitation functions for light-ion induced reactions. The calculated values were obtained from the empirical rule on excitation functions (Hata/47/).

of shell structure.

Some results of calculations by STAPRE code has been presented by Pavlik in Wien group in the same meeting above mentioned/48/. The incident are protons and alpha-particles covering the incident energy up to 30 MeV and targets are also in the mass region around 50. He has mentioned, if STAPRE code is carefully used for proton and alpha-particle induced reactions with incident particle energies up to 40 to 50 MeV, that calculated results with uncertainties of 30% seem possible. For global parameter sets for a gross estimate of an unknown excitation functions, an estimation within a factor of about two is possible.

Conclusion

Nuclear structure and reaction cross section and yield data which are related to some radioisotopes for medical use were examined and came to the following conclusions. (1) For several radioisotopes such as ^{64}Ga , ^{124}I and ^{123}Xe , more precise determinations of absolute gamma-ray emitting probabilities are necessary. (2) Cross section data for several medical radioisotopes are well examined. However, in some cases more experimental measurements are needed. (3) The monitor reactions should be documented and evaluation is desirable. (4) The number of isotopes applied to the medicine is still increasing. The new techniques, such as projectile fragmentation of high energy heavy ions and fast neutron reactor, to produce more wide region of radioisotopes are developing. This would serve to introduce new kind of isotopes application in nuclear medicine.

References

1. A.J.Palmer and D.M.Taylor, edited, 'Radio-pharmaceuticals labelled with Halogen Isotopes': Int.J.Appl.Radiat.Isot.37, No.8(1986).
2. S.M.Qaim: Radiochim.Acta 30,147(1982).
3. S.L.Waters: INDC(NDS)-195/GZ,37(1988).
4. A.B.Whitehead and I.S.Foster: Canad.J.Phys, 36,1276(1958).
5. M.Furukawa, Y.Ishizaki, Y.Nakano, T.Nozaki, Y.Saji and S.Tanaka: J.Phys.Soc.Japan 15,2167(1960).

6. W.Gruhle and B.Kober: Nucl.Phys., **A286**, 523(1977).
7. R.H.McCamis, G.A.Moss and J.M.Cameron: Can.J. Phys., **51**, 1689(1973).
8. M.C.Lagunas-Solar, O.F.Carvacho and R.R.Cima: Int.J.Appl.Radiat.Isot., **39**, 41 (1988).
M.C.Lagunas-Solar: INDC(NDS)-195/GZ, 55 (1988).
9. M.C.Shaeffler, F.Barreto, J.R.Datesh, B.R.Goldstein: ORNL/MIT-258(1977).
10. B.W.Wieland and R.R.Highfill: IEE Transactions on Nucl.Sci., NS-26, 1713 (1979).
11. K.Suzuki, Radioisotopes: **34**, 537(1985) (in Japanese).
12. R.Michel, G.Brinkmann, H.Weigel and W.Herr: Nucl.Phys., **A322**, 40(1979).
13. B.L.Cohen and T.H.Handley: Phys.Rev., **93**, 514(1954).
14. I.R.Williams and C.B.Fulmer: Phys.Rev., **162**, 1055(1967).
15. R.A.Sharp, R.M.Diamond and G.Wilkinson: Phys.Rev., **101**, 1493(1956).
16. S.Tanaka, M.Furukawa and M.Chiba: J.Inorg.Nucl.Chem., **34**, 2419(1972).
17. M.W.Greene, E.Lebowitz, P.Richards and M.Hillman: Int.J.Appl.Radiat.Isot., **21**, 719(1970).
18. R.Michel and G.Brinkmann: Nucl.Phys., **A338**, 167(1980).
19. S.Tanaka, M.Furukawa, S.Iwata, M.Yagi, H.Amano and T.Mikumo: J.Phys.Soc.Japan, **15**, 1547(1960).
20. J.Jastrzebski: Phys.Rev., **C19**, 724(1979).
21. Z.Kovacs, G.Blessing, S.M.Quaim and G.Stocklin: Int.J.Appl.Radiat.Isot., **36**, 635(1985).
22. S.R.Wilkins, S.T.Shimose, H.H.Hines, J.A.Jungerman, F.Hegedus: Int.J.Appl.Radiat.Isot. **26**, 279(1975).
23. A.M.J.Paans, W.Vaalburg, G.van Herk and M.G.Woldring: Int.J.Appl.Radiat.Isot. **27**, 465 (1976).
24. M.Diksic and L.Yaffe: J.Inorg.Nucl.Chem., **39**, 1299(1977).
25. D.B.Syme, E.Wood, I.M.Blair, S.Kew, W.Perry and P.Cooper: Int.J.Appl.Radiat.Isot., **29**, 29 (1978).
26. M.C.Lagunas-Solar, O.F.Carvacho, L.J.Harris and C.A.Mathis: Int.J.Appl.Radiat.Isot., **37**, 827(1986).
27. K.Kondo, R.M.Lambrech, E.F.Norton and A.P.Wolf: Int.J.Appl.Radiat.Isot., **28**, 765(1977).
28. R.Weinreich, O.Schult and G.Stocklin: Int. J.Appl.Radiat.Isot., **25**, 535((1974).
29. J.B.Cumming: Ann.Rev.Nucl.Sci. **13**, 261(1963).
30. M.Diksic and L.Yaffe: J.Inorg.Nucl.Chem., **39**, 1299(1977).
31. P.M.Grant, D.A.Miller, J.S.Gilmore and H.A.O'Brien, Jr.: Int.J.Appl.Radiat.Isot., **33**, 415(1982).
32. C.Wasilevsky, M.V.Vedoya and S.J.Nassiff: Int.J.Appl.Radiat.Isot., **37**, 319(1986).
33. T.Horiguchi, H.Noma, Y.Yoshizawa, H.Takemi, H.Hasai, Y.Kiso: Int.J.Appl.Radiat.Isot., **31**, 141(1980).
34. R.Weinreich and J.Knieper: Int.J.Appl.Radiat. Isot., **34**, 1335(1983).
35. A.M.J.Paans, J.Welleweerd, W.Vaalburg, S.Reifferses and M.G.Woldring: Int.J.Appl. Radiat.Isot., **31**, 267(1980).
36. T.Horiguchi, H.Kumahora, H.Inoue and Y.Yoshizawa: Int.J.Appl.Radiat.Isot., **34**, 1531 (1983).
37. S.M.Quaim, H.Ollig and G.Blessing: Int.J.Appl. Radiat.Isot. **33**, 271(1982).
38. J.H.Zaidi, S.M.Quaim and G.Stocklin: Int.J. Appl.Radiat.Isot. **34**, 1425(1983).
39. H.Youfeng, S.M.Quaim and G.Stocklin: Int.J.Appl.Radiat.Isot., **33**, 13(1982).
40. A.Hashizume: INDC(NDS)-195/GZ, 44(1983).
41. G.J.Beyer, A.F.Novgorodov, F.Roesch and H.L.Ravn: INDC(NDS)-195/GZ, 77(1988).
42. I.F.Goncalves, Zs.Schram, Z.Papp and S.Darczy: Int.J.Appl.Radiat.Isot., **38**, 989 (1987).
43. K.Masumoto, T.Kato and N.Suzuki: Nucl.Instr. and Meth., **157**, 567(1978).
44. J.Heizl, E.Huenges and H.Morinaga: INDC(NDS) -195/GZ, 71(1988).
45. M.Blann: INDC(NDS)-195/GZ, 115(1988).
46. R.Michel, F.Peiffer and R.Stuck: Nucl.Phys., **A441**, 617(1985).
47. K.Hata and H.Baba: INDC(NDS)-195/GZ, 131 (1988).
48. A.Pavlik: INDC(NDS)-195/GZ, 124(1983).